Catal Lett (2008) 120:154–160
DOI 10.1007/s10562-007-9268-5

Characterization of Acidity and Porosity of Zeolite Catalysts by the Equilibrated Thermodesorption of n-Hexane and n-Nonane

Wacław Makowski · Barbara Gil · Dorota Majda

Received: 13 June 2007 / Accepted: 4 September 2007 / Published online: 21 September 2007

Abstract Thermodesorption of n-hexane and n-nonane from the acidic and non-acidic zeolites ZSM-5 and Y was studied by means of the thermogravimetric temperature programmed equilibrated desorption (TPED) and quasi-equilibrated temperature programmed desorption and adsorption (QE-TPDA). Micropore volumes determined from the adsorption capacity of n-hexane were close to those determined by N_2 adsorption. Content and strength of acid sites in the acidic zeolites estimated by fitting the Arrhenius equation to the high temperature parts of QE-TPDA profiles of n-hexane attributed to its cracking were in agreement with their acidity characteristics obtained by IR spectroscopy of chemisorbed pyridine. The mesopore volume was determined from the QE-TPDA profiles of n-nonane. Coking observed only for QE-TPDA of n-nonane on H-USY zeolite resulted in blocking the micropores without affecting the mesopores.

Keywords Thermodesorption · Zeolites · n-Hexane · n-Nonane · Pore volume · Acidity

1 Introduction

Adsorption of n-alkanes may be employed for characterization of porosity of various porous materials. The micropore volume of zeolites may be determined from the saturation sorption capacity of n-hexane [1]. Temperature programmed desorption of n-nonane was proposed as a comparative method for estimation of micropore size in zeolites and carbon molecular sieves [2]. The effective pore sizes in zeolites may be also assessed from the correlation between the adsorption enthalpy and entropy of various n-alkanes [3].

In our earlier papers we demonstrated that the equilibrated thermodesorption, either monitored gravimetrically under constant partial pressure of the adsorptive (TG-TPED) [4, 5, 6] or measured under quasi-equilibrium conditions in a standard TPD apparatus (QE-TPDA) [6, 7, 8], is a good method for studying adsorption n-alkanes in zeolites and mesoporous molecular sieves. It may be employed as a method for characterization of their porous structure, yielding not only the micropore volume and the adsorption enthalpy and entropy, but also revealing phase transitions due to ordering of the molecules adsorbed in the micropores that are closely related to geometry of the micropore systems [9]. Evidences of such transitions were observed for MFI [5], MEL [5], FER [10], BEA [11], LTA [11] and LTL [11] type structures. In the case of n-nonane, the equilibrated thermodesorption profiles exhibit also effects resulting from desorption of the molecules filling the mesopores, allowing determination of the mesopore volume and size [8].

Strong acid sites present inside the micropores of acidic zeolites may affect adsorption and desorption of hydrocarbon molecules, either by direct interactions or by catalyzing their isomerization, cracking or reactions leading to coke formation. In our preliminary studies on highly acidic zeolites studies we observed such catalytic transformation only for n-nonane [8]. In this work possibility of application the equilibrated thermodesorption of n-hexane

W. Makowski (✉) · B. Gil
Faculty of Chemistry, Jagiellonian University, Ingardena 3, Krakow 30-060, Poland
e-mail: makowski@chemia.uj.edu.pl

D. Majda
Regional Laboratory for Physicochemical Analyses and Structural Research, Jagiellonian University, Ingardena 3, Krakow 30-060, Poland
e-mail: majda@chemia.uj.edu.pl

and n-nonane for characterization of both acidity and porosity of acidic zeolite catalysts was explored.

2 Experimental

Acidic zeolites HZSM-5 (Zeolyst, Si/Al = 15) and USY (ultra stabilized HY—Linde LZY-82, global Si/Al = 3.0, framework Si/Al = 4.5 [12]), both delivered in ammonia-exchanged forms as well as non-acidic (high silica) zeolites HZSM-5 (Zeolyst, Si/Al = 140) and HY (Degussa, Si/Al > 100) were used in this study. Acidic zeolites were also studied after neutralization by short treatment with excess of 0.08 M NaOH solution in ethanol, followed by drying. Analytical pure n-hexane (POCh, Poland) and 99% n-nonane (Laborchemie Apolda, Germany) were used as sorbates.

Quasi-equilibrated temperature programmed desorption and adsorption (QE-TPDA) experiments were performed using a homemade temperature programmed desorption setup equipped with a thermal conductivity detector that was described in detail earlier [7, 8]. Prior the QE-TPDA experiments a sample (ca. 10 mg) was activated by heating in a flow of pure He to 500 °C at 10 °C/min and then cooled down. After the activation adsorption at room temperature was started, by replacing He flowing through the sample cell with of He/hydrocarbon (HC) mixture (0.3–0.5 vol%). When adsorption was completed and the detector signal stabilized, the QE-TPDA experiment was performed by heating the sample with the preadsorbed HC in the flow of He/HC mixture (7.5 cm^3/min) according to a temperature program consisting of a heating and cooling ramp (5 or 10 °C/min, high temp. limit 500 or 600 °C). Such desorption–adsorption cycles followed by isothermal segments (60 min at room temperature) were repeated several times.

In the gravimetric measurements of the temperature programmed equilibrated desorption (TPED) of n-hexane a standard thermobalance (Mettler-Toledo TGA/SDTA 851^e) was used. The carrier gas (Ar) was saturated with of n-hexane vapors at 0 °C, thus the measurements were performed at the constant partial pressure of the adsorptive (0.06 bar). After the activation of the sample and sorption in situ, the thermodesorption measurement was performed by heating the sample to 400 °C at the constant rate of 5 °C/min. Details of the TPED measurements were published elsewhere [4, 5]

IR spectroscopy of the acidic –OH groups and of the chemisorbed pyridine was additionally applied for characterization of the acidity of the studied zeolites. IR spectra were recorded by Bruker Equinox 55 spectrometer quipped with an MCT detector. For IR studies the zeolites were pressed into thin wafers and activated in situ in the IR cell under vacuum at 500 °C. The temperature of pyridine adsorption was 170 °C and desorption was performed by gradual increasing the temperature.

3 Results

Thermodesorption profiles of n-hexane obtained for acidic and non acidic zeolites ZSM-5 and Y in the QE-TPDA measurements are shown in Fig. 1. These profiles, with two desorption maxima for ZSM-5 and with one desorption maximum for Y type zeolites are in agreement with the previous findings [4, 7]. The low temperature peaks in the profiles observed for ZSM-5 result from the commensurate freezing effect i.e. an order-disorder transition in the adsorbed phase occurring at adsorption degree (above 50% of maximum sorption capacity) [9]. Excellent reproducibility of the QE-TPDA profiles obtained in following desorption–adsorption cycles indicates that the adsorptive properties of the zeolites related to their microporous structure do not change during the experiments.

The profiles observed for the acidic zeolites differ from those obtained for the non-acidic ones. These differences should be attributed to transformations of n-hexane molecules catalyzed by the acid sites. Increased detector signal at high temperatures indicates higher total concentration of hydrocarbons in the carrier gas due to cracking of n-hexane. This increase is higher for HZSM-5 (15) because

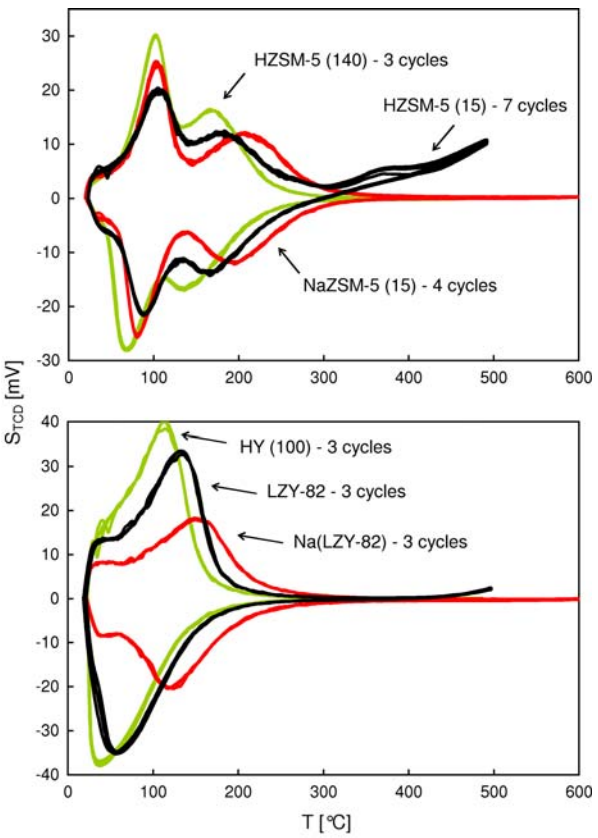

Fig. 1 QE-TPDA profiles of n-hexane for acidic, neutralized and non-acidic zeolites ZSM-5 and Y, observed in several consecutive desorption–adsorption cycles (heating/cooling rate 10 °C/min)

of its higher acidity. A small maximum observed for this zeolite in the desorption profile at 375 °C most probably results from thermal decomposition of reactive carbon deposits that are intermediates in the cracking of n-hexane.

The QE-TPDA profiles of n-hexane depend on both the Si/Al ratio and type of the extraframework cations. Neutralization of HZSM-5 (15) or LZY-82 not only totally eliminates all the effects attributed to the acid sites, but also shifts positions of the desorption/adsorption peaks to higher temperatures. On the other hand, for non-acidic zeolites HZSM-5 (140) and HY (100) these peaks appear at considerably lower temperatures. Such dependence indicates that interactions of n-hexane molecules with Na^+ cations and Al framework atoms play a role in its adsorption in the zeolite's micropores.

The thermodesorption profiles of n-hexane obtained for ZSM-5 zeolites in thermogravimetric measurements under equilibrium conditions (TG-TPED) shown in Fig. 2 are in agreement with the QE-TPDA results. While the profiles obtained for the non-acidic zeolite are almost identical, the differences in those obtained for the acidic zeolite result mainly from different conditions and principles of the measurements. A sharp increase observed in the DTG-TPED profile at 210 °C is an evidence of formation of the carbonaceous reaction intermediates. Because of higher partial pressure of the adsorptive such a formation of the intermediates of occurs at lower temperatures. It should be mentioned that apart from cracking also isomerization of n-hexane is catalyzed by the acid sites. Since the latter reaction may be not detected in QE-TPDA experiments, the results observed for acidic zeolites in two types of experiments are not fully equivalent.

The QE-TPDA profiles of n-nonane shown in Fig. 3 are consistent with those observed for n-hexane. The high temperature peaks result from desorption and adsorption in the micropores, while in the low temperature region additional peaks related to capillary condensation in the mesopores appear [8]. For ZSM-5 zeolites the low temperature peaks may contain also a contribution of the commensurate freezing effects. For ZSM-5 (15) zeolites only one desorption maximum was observed in the low temperature region but for all the other zeolites there two distinct maxima could be detected. Evident desorption–adsorption hysteresis

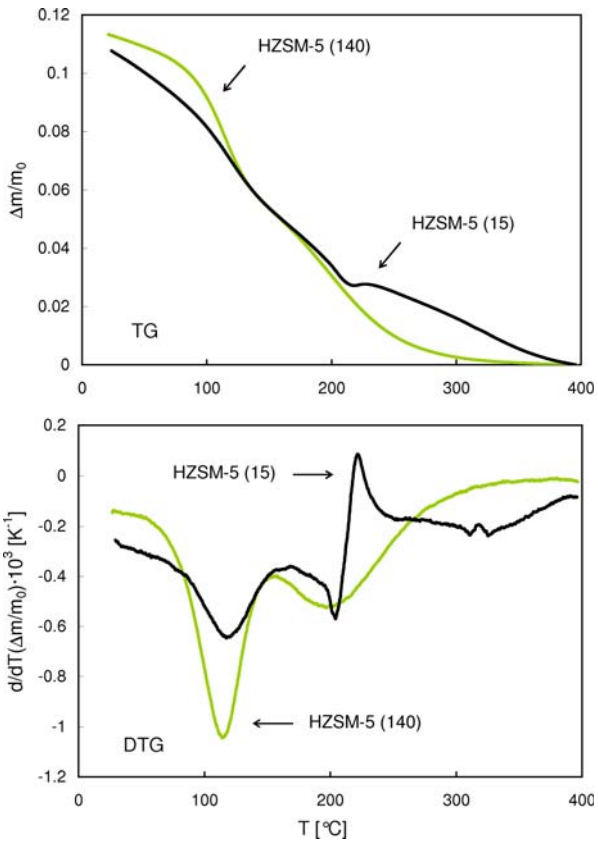

Fig. 2 Thermodesorption profiles of n-hexane measured under the constant partial pressure (0.06 bar) by TGA for acidic and non-acidic zeolites ZSM-5 (heating rate 5 °C/min)

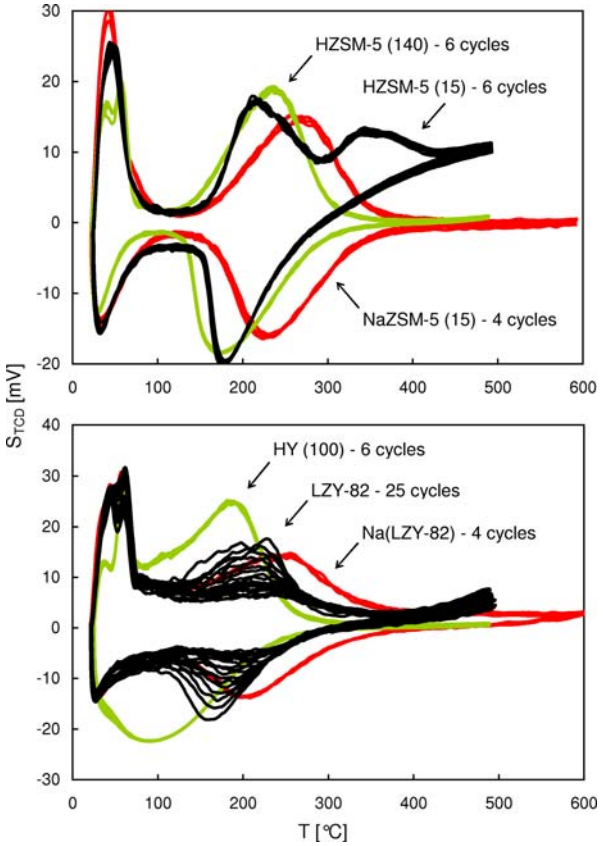

Fig. 3 QE-TPDA profiles of n-nonane for acidic, neutralized and non-acidic zeolites ZSM-5 and Y, observed in several consecutive desorption–adsorption cycles (heating/cooling rate 10 °C/min). For clarity of the plot the first desorption–adsorption profile for HZSM-5 (15), exhibiting an irreproducible peak at ca 200 °C [8] (attributed to desorption of the molecules chemisorbed on the acid sites) was omitted

indicates that the second maximum should be attributed to desorption from the mesopores. The nature of the first maximum is less clear—apart from the commensurate freezing it may be related with larger (e.g. interparticle) mesopores or multilayer adsorption at the external surface of the zeolitic crystallites.

Because n-nonane is more prone for cracking, the effects of the zeolites' acidity are more noticeable—the increase of the detector signal at high temperatures as well as the intensity of the maximum observed for HZSM-5 (15) at 350 °C are higher than for n-hexane. While the profiles observed in consecutive desorption adsorption cycles for HZSM-5 (15) are practically the same, those obtained for LZY-82 reveal gradual decline of the adsorption capacity. This should be attributed to coke formation in the micropore leading to a decrease of their volume. Interestingly, the mesopores (represented by the low temperature desorption peaks) seem to be not affected by coking.

The influence of the Si/Al ratio and extraframework cations on QE-TPDA profiles of n-nonane is the same as that observed for n-hexane. Neutralization of the acidic zeolites completely suppresses cracking and coking, and results in a shift of the desorption/adsorption peaks to the higher temperatures.

4 Discussion

The increased detector signal observed in the QE-TPDA profiles at high temperatures for acidic zeolites was attributed to cracking of n-alkanes. It was assumed that this increase was proportional to the reaction rate and the linearized Arrhenius equation was fitted to the transformed experimental data for n-hexane. Results of the fitting is shown in Fig. 4 and the fitted parameters of the Arrhenius equitation are listed in Table 1. Lower pre-exponential factor obtained for HZSM-5 (15) indicates that this zeolite contains less acid sites than LZY-82. However, lower activation energy observed for HZSM-5 (15) reveals higher strength (i.e. cracking activity) of the acid sites in this zeolite. These results are confirmed by those obtained form IR spectra of pyridine chemisorbed on Bronsted acid sites (1,545 cm^{-1}), also showing higher strength and lower content of the acid sites in HZSM-5 (15) than in LZY-82.

Adsorption of n-alkanes on zeolites is often quantified using functions derived from the Langmuir model [13, 14, 15]. Single step profiles are fitted with simple Langmuir isotherms or isobars, but for two step profiles (typical for zeolites ZSM-5) usually dual site Langmuir (DSL) functions are used. Generally good agreement is observed at low adsorption degrees. Deviations of the experimental profiles form the model are attributed to sorbate-sorbate interactions [16] or multilayer adsorption et the external surface of the zeolite crystallites. Values of the adsorption enthalpy and entropy determined by fitting the Langmuir model function usually do not differ considerably from those determined using other methods [7 and the references therein]

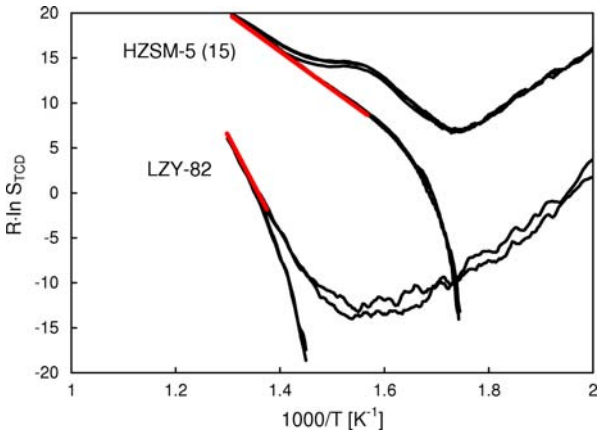

Fig. 4 Fitting the Arrhenius equation to the high temperature parts of the QE-TPDA profiles of n-hexane for acidic zeolites, attributed to the catalytic cracking

Table 1 Parameters characterizing acidity of zeolites determined from QE-TPDA profiles of n-hexane and IR spectra of the adsorbed pyridine

Zeolite	Cracking of n-hexane		IR of chemisorbed pyridine	
	ln A[a]	E_{act}[b] [kJ/mol]	N_{H+}/u.c.[c]	A_{450}/A_{170}[d]
HZSM-5 (15)	75	42	2.4	0.851
LZY-82	151	111	14.5	0.688

[a] preexponential factor

[b] activation energy

[c] number of Bronsted acid sites per unit cell

[d] relative strength of acid sites i.e. the ratio of absorbances of pyridine chemisorbed on Bronsted sites at 450 °C and 170 °C [12]

From the QE-TPDA data approximate adsorption isobars $\theta(T)$ may be determined by averaging of the integrated desorption and adsorption profiles [11].

$$\theta(T) = 1 - \frac{A(T_0, T)}{A(T_0, T_f)} \quad (1)$$

where

$$A(T_0, T) = \int_{T_0}^{T} S_{TCD} dT \quad (2)$$

T is temperature, T_0 and T_f denote the beginning and the end of the thermodesorption peak. Temperature for a given adsorption degree θ is calculated a mean value of the desorption and adsorption temperature

$$T_\theta = \frac{(T_{des})_\theta + (T_{ads})_\theta}{2} \quad (3)$$

Example of such an averaging for n-hexane on HZSM-5 (15) is shown in Fig. 5. Integration of the QE-TPDA profiles was limited to temperatures below 300 °C, so that their high temperature parts attributed to cracking of n-hexane were omitted.

Temperature derivatives of the adsorption isotherms were fitted with functions derived from the Langmuir model

$$\frac{d\theta}{dT} = \frac{\Delta H_{ads} p \exp\left(-\frac{\Delta G_{ads}}{RT}\right)}{\left[1 + p\exp\left(-\frac{\Delta G_{ads}}{RT}\right)\right]^2 RT^2} \quad (4)$$

where p is the relative partial pressure of the adsorptive ($p = p_i/p^\circ$) in the carrier gas, $\Delta G_{ads} = \Delta H_{ads} - T\Delta S_{ads}$ and ΔH_{ads} and ΔS_{ads} are the adsorption enthalpy and entropy. Examples of the fitting the models functions to the differential isotherms of n-hexane on the studied acidic zeolites are shown in Fig. 6. In the case of HZSM-5 a differential DSL function (being a linear combination of two terms given by Eq. 4) was used. Good agreement between the experimental and the model profiles was observed for temperatures above 90 °C.

Values of the adsorption enthalpy and entropy obtained by fitting the model functions are listed in Table 2. Initial adsorption heat ranges form 58 to 64 kJ/mol for zeolites Y and from 60 to 70 kJ/mol for ZSM-5. However, for the latter zeolite much higher adsorption heat (79–110 kJ/mol) was computed for the low temperature peaks (i.e. high adsorption degree). Judging from the ΔH_{ads} and ΔS_{ads} values it is difficult to rationalize the shifts of the thermodesorption peaks' positions after neutralization—while for ZSM-5 (15) the origin of the shift seems an increase in the adsorption heat, for LZY-82 it is rather a decrease in the adsorption entropy loss. On the other hand, the differences in the peak positions observed for the acidic and high-silica zeolites are clearly related to entropy effects. Higher values of the adsorption entropy loss ($-\Delta S_{ads}$) found for the high-silica zeolites indicate higher degree of ordering of the adsorbed molecules that may be attributed to better crystallinity, expected for higher Si/Al ratios.

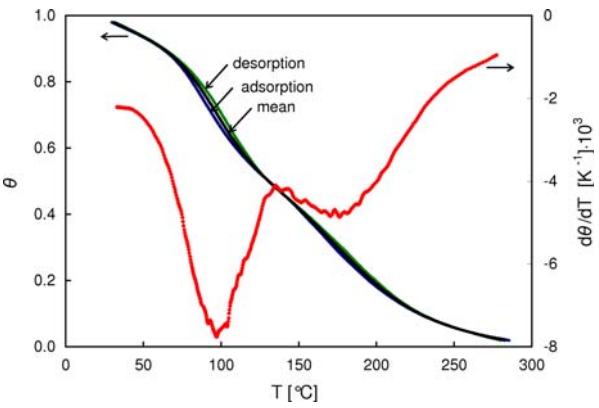

Fig. 5 Adsorption isobar of n-hexane on HZSM-5 (15) determined by averaging the integrated desorption and adsorption profiles and its temperature derivative (heating/cooling rate 5 °C/min)

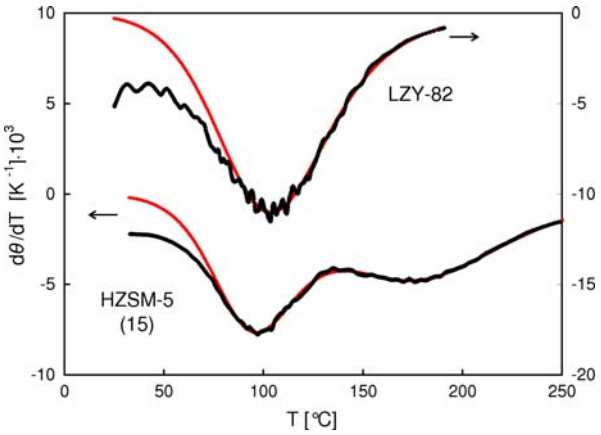

Fig. 6 Examples of fitting the Langmuir and DSL functions to the differential adsorption isobars of n-hexane on acidic zeolites

Table 2 Values of the adsorption enthalpy and entropy determined from QE-TPDA profiles of n-hexane

Zeolite	$-\Delta H_{ads}$ [kJ/mol]		$-\Delta S_{ads}$ [J/(mol K)]	
HZSM-5 (15)[a]	79[c]	60[d]	172[c]	88[d]
HZSM-5 (15)[b]	–	–	–	–
NaZSM-5 (15)[a]	91[c]	66[d]	204[c]	95[d]
HZSM-5 (140)[a]	110[c]	70[d]	260[c]	117[d]
HZSM-5 (140)[b]	104[c]	64[d]	247[c]	110[d]
LZY-82[a]	63		122	
Na(LZY-82)[a]	58		98	
HY (100)[a]	64		133	

[a] measured by QE-TPDA

[b] measured by TG-TPED

[c,d] peak position ([c]low temperature peak, [d]high temperature peak)

Values of the saturation adsorption capacity of n-hexane and n-nonane and the pore volumes are listed in Table 3. The latter values were computed from the adsorption capacity data obtained by integration of the QE-TPDA profiles, assuming that density of the adsorbed hydrocarbon was the same as that of the liquid. The initial sample mass was corrected for moisture content determined by TGA measurements. In the case of n-nonane the QE-TPDA profiles were divided into two parts corresponding to desorption from the mesopores and micropores.

The micropore volumes determined for the acidic zeolites are slightly lower than the literature data of 0.16–0.17 cm^3/g for ZSM-5 [4, 17, 18], 0.28–0.29 cm^3/g for

Table 3 Values of the saturation sorption capacity and pore volumes determined by the equilibrated thermodesorption of n-hexane and n-nonane

Zeolite	n-hexane		n-nonane			
	$\Delta m/m_0^c$ [mg/g]	V_{micro}^d[cm^3/g]	$\Delta m/m_0^c$ [mg/g]	V_{pore}^e[cm^3/g]		
				V_{total}	V_{meso}	V_{micro}
HZSM-5 (15)[a]	96	0.145			0.053	
HZSM-5 (15)[b]	108	0.163				
NaZSM-5 (15)[a]	93	0.140	131	0.181	0.062	0.119
HZSM-5 (140)[a]	112	0.169	130	0.180	0.048	0.133
HZSM-5 (140)[b]	113	0.172				
LZY-82[a]	147	0.222	216	0.300	0.068	0.232
Na (LZY-82)[a]	146	0.221	228	0.316	0.072	0.244
HY (100)[a]	176	0.266	199	0.277	0.015	0.262

[a] measured by QE-TPDA

[b] measured by TG-TPED

[c] saturation sorption capacity

[d] pore volume, determined from the saturation sorption capacity

[e] micropore volume $V_{micro} = V_{total} - V_{meso}$

USY [19] and 0.32–0.34 cm^3/g for Y [4, 19] obtained from N_2 adsorption isotherms, but the same values were obtained for high-silica ZSM-5. The micropore volume found for HY (100) is lower than the N_2 adsorption value. This may indicate that N_2 molecules more efficiently fill the micropore volume than n-hexane molecules, especially in the case of FAU structure comprised of large supercages. However, the actual density of n-hexane adsorbed in ZSM-5 may be higher than in other zeolites due to ordering of the molecules in MFI structure.

Practically the same micropore volumes obtained for HZSM-5 (140) from TG-TPED and QE-TPDA measurements confirm validity of calibration used in the latter experiments. Differences in the micropore volume between the acidic and high-silica zeolites may result from framework distortions that are more probable for high-alumina ZSM-5 and steamed Y zeolites or form variation of moisture content in these zeolites depending on storage conditions.

Values of the micropore volume determined from the QE-TPDA profiles of n-nonane are only slightly larger than those obtained by thermodesorption of n-hexane for zeolites Y, but they are smaller for ZSM-5 probably because of relatively lower density of the adsorbate than in the case of n-hexane (since for n-nonane the commensurate freezing phase transition is not completed at room temperature).

Changes of the micro- and mesopore volume observed for LZY-82 in the QE-TPDA of n-nonane are shown in Fig. 7. While the micropore volume decreases quickly with following desorption/adsorption cycles, the mesopore volume hardly changes even for very high value of the upper temperature limit. This indicates the coking of USY due to

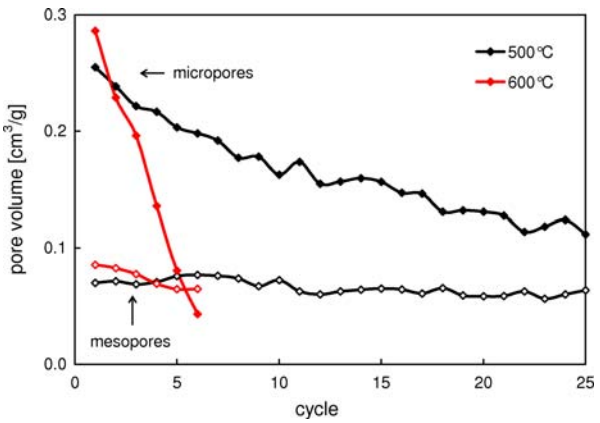

Fig. 7 Evolution of the micro- and mesopore volume in the QE-TPDA cycles of n-nonane on LZY-82 (heating/cooling rate 10 °C/min, final temperature 500 or 600 °C)

the cracking of n-nonane is limited to the micropores, but does not affect the mesopores.

IR spectroscopy was employed for characterization of the acidic properties of the fresh and partially coked (i.e. after one desorption cycle) LZY-82 zeolite. Comparison of spectra presented in Fig. 8 indicate that all bands attributed to the acidic -OH groups disappear after short coking. However, the spectra of chemisorbed pyridine (Fig. 9) show that content and availability of the acid sites in these zeolites is practically the same. This means that although the coke strongly interacts with the acidic hydroxyl groups, changing their spectroscopic characteristics, they remain available to pyridine or n-nonane molecules. Similar effect was observed before [20] and the mechanism of poisoning by coke seems to depend on the coke coverage [21]. At low

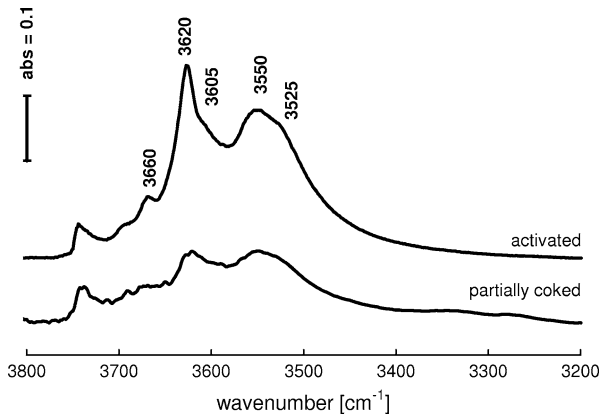

Fig. 8 IR spectra of OH groups in the activated and partially coked LZY-82 zeolite. Wavenumbers of the bands characteristic for the acidic –OH grups [12] are indicated in the figure

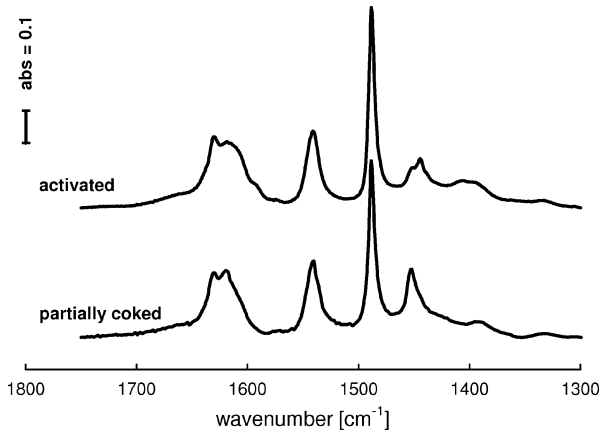

Fig. 9 IR spectra of adsorbed pyridine on the activated and partially coked LZY-82 zeolite

coke loading (ca 6 wt%) zeolite's acid sites are directly blocked by coke molecules, while at higher loading deactivation is additionally realized by a pore blockage. For the first case interaction between acidic proton and weakly basic coke caused disappearance of the band of free acidic OH groups at 3,620 and 2,605 cm⁻1. Nevertheless, these OH groups are still available to pyridine, as it displaces weakly basic coke from the acid sites, forming much stronger complex—pyridinium ions. For much weaker base, ammonia, the displacement effect does not take place [22].

5 Conclusions

It has been demonstrated that quasi equilibrated temperature programmed desorption and adsorption of n-hexane and n-nonane may be applied for characterization of acidic zeolites catalysts. QE-TPDA of n-hexane allows determination of the micropore volume and the adsorption enthalpy and entropy, and as well as assessment of the content and strength of the acid sites. From QE-TPDA of n-nonane the mesopore volume may be obtained. All the effects related to the zeolites' acidity may be eliminated by their simple neutralization.

Acknowledgement This work has been supported by the Ministry of Science and Higher Education of Poland with a grant number N507 108 32/3175

References

1. Ruthven DM (2001) In: Robson H (ed) Verified syntheses of zeolitic materials. Elsevier, Amsterdam, pp 61–65
2. Mittelmeijer-Hazeleger MC, van der Linden B, Bliek A (1995) J Porous Mater 2:25
3. Jentys A, Lercher JA (2001) In: van Bekkum H, Jacobs PA, Flanigen EM, Jansen JC (eds) Introduction to zeolite science and practice. Elsevier, Amsterdam, p 357
4. Makowski W, Majda D (2004) Thermochim Acta 412:131
5. Makowski W, Majda D (2005) Appl Surf Sci 252:707
6. Makowski W, Majda D (accepted) J Porous Mater (doi:10.1007/s10934-006-9004-3)
7. Makowski W (2007) Thermochim Acta 454:26
8. Makowski W, Kuśtrowski P (2007) Micropor Mesopor Mater 102:283
9. Smit B, Maesen TLM (1995) Nature 374:42
10. Majda D, Makowski W (2005) Stud Surf Sci Catal 158:1161
11. Makowski W, Ogorzałek Ł, Thermochim Acta, submitted
12. Datka J, Gil B, Złamaniec J, Batamack P, Fraissard J, Massiani P (1999) Polish J Chem 73:1535
13. Millot B, Methivier A, Jobic H (1998) J Phys Chem 102:3210
14. Gribov EN, Sastre G, Corma A (2005) J Phys Chem B 109:23794
15. Zhu W, Kapteijn F, van der Linden B, Moulijn JA (2001) Phys Chem Chem Phys 3:1755
16. Eder F, Lercher JA (1997) Zeolites 18:75
17. Tao Y, Kanoh H, Kaneko K (2006) Adsorption 12:309
18. Groen JC, Peffer LAA, Moulijn JA, Pérez-Ramìrez J (2004) Coll Surf A Physicochem Eng 241:53
19. Denayer JF, Baron GV, Jacobs PA, Martens JA (2000) Phys Chem Chem Phys 2:1007
20. Cerqueira HS, Ayrault P, Datka J, Guisnet M (2000) Micropor Mesopor Mater 38:197
21. Cerqueira HS, Ayrault P, Datka J, Magnoux P, Guisnet M (2000) J Catal 196:149
22. Gil B, Mierzyńska K, Szczerbińska M, Datka J (2007) Micropor Mesopor Mater 99:328